Structural and magnetic properties of the 5d^{2} double perovskites Sr_{2}BReO_{6} (B=Y, In)

A. A. Aczel, Z. Zhao, S. Calder, D. T. Adroja, P. J. Baker, and J.-Q. Yan

Phys. Rev. B **93**, 214407 — Published 7 June 2016

DOI: 10.1103/PhysRevB.93.214407

Structural and magnetic properties of the $5d^2$ double perovskites Sr_2BReO_6 ($B = $ Y, In)

A. A. Aczel,[1,*] Z. Zhao,[2,3] S. Calder,[1] D.T. Adroja,[4,5] P.J. Baker,[4] and J.-Q. Yan[2,6]

[1]*Quantum Condensed Matter Division, Oak Ridge National Laboratory, Oak Ridge, TN 37831, USA*
[2]*Materials Science and Technology Division, Oak Ridge National Laboratory, Oak Ridge, TN 37831, USA*
[3]*Department of Physics and Astronomy, University of Tennessee, Knoxville, Tennessee 37996, USA*
[4]*ISIS Facility, STFC Rutherford Appleton Laboratory, Harwell Oxford, Oxfordshire, OX11 0QX, UK*
[5]*Highly Correlated Matter Research Group, Physics Department,*
University of Johannesburg, P.O. Box 524, Auckland Park 2006, South Africa
[6]*Department of Materials Science and Engineering, University of Tennessee, Knoxville, Tennessee 37996, USA*

(Dated: May 19, 2016)

We have performed magnetic susceptibility, heat capacity, neutron powder diffraction, and muon spin relaxation experiments to investigate the magnetic ground states of the $5d^2$ double perovskites Sr_2YReO_6 and Sr_2InReO_6. We find that Sr_2YReO_6 is a spin glass, while Sr_2InReO_6 hosts a non-magnetic singlet state. By making detailed comparisons with other $5d^2$ double perovskites, we argue that a delicate interplay between spin-orbit coupling, non-cubic crystal fields, and exchange interactions plays a key role in the great variation of magnetic ground states observed for this family of materials.

PACS numbers: 75.25.-j, 75.30.Cr, 75.40.Cx, 75.50.Lk, 75.70.Tj, 76.75.+i

I. INTRODUCTION

Transition metal compounds containing heavy $5d$ atoms are often governed by spin-orbit coupling (SOC), electronic correlations, and crystal field effects of comparable strength [1]. The relativistic entanglement of correlated orbital and spin degrees of freedom in such materials can drive exotic quantum states of matter, such as effective $J = 1/2$ Mott insulators [2], topological superconductors and insulators [3–6], and quantum spin liquids [7]. The research community has placed a great deal of emphasis on $5d^5$ systems due to the extreme quantum nature of the novel effective $J = 1/2$ state associated with that particular d-electron configuration. On the other hand, far less work has focused on $5d^1$-$5d^4$ materials even though strong SOC may play a key role in determining their magnetic properties.

Double perovskites (DPs) of the form $A_2BB'O_6$, with magnetic $4d$ or $5d$ B' ions, provide an outstanding opportunity to investigate the interplay of SOC, structural distortions, and d-electron configuration on the magnetism of the geometrically-frustrated face-centered-cubic (fcc) lattice [8]. Hundreds of DPs have now been synthesized in polycrystalline form, and subsequent characterization work revealed a diverse array of magnetic properties. The $5d^5$ DPs that have been studied in detail, including La_2MgIrO_6 and La_2ZnIrO_6, are effective $J = 1/2$ candidates [9] that exhibit antiferromagnetic ground states and interesting magnetic excitations [10, 11]. Materials composed of magnetic ions with $4d^3$/$5d^3$ electron configurations generally host ordered magnetic ground states also [12–17], aside from a few known exceptions [18, 19]. Historically, it has been argued that the spin arrangements in these systems are well-accounted for by mean field theory, with ground state selection arising from the signs and magnitudes of the nearest neighbor and next nearest neighbor exchange interactions [20], although this simple hypothesis has been challenged recently [21]. On the other hand, the magnetic order of $4d^3$/$5d^3$ and $5d^5$ systems often gives way to exotic magnetic states in $4d^1$/$5d^1$ quantum spin DPs. For example, Ba_2YMoO_6 has been described as a valence bond glass with a collective spin-singlet ground state [22, 23] and Sr_2BReO_6 ($B = $ Mg, Ca) are best characterized as unconventional spin glasses, since no obvious source of disorder has been found [24–26].

The magnetism of heavy metal d^2 DPs serves as an interesting intermediate case between the d^1 and d^3/d^5 analogues, and recent theoretical work has established a phase diagram for the cubic limit [27]. While there are currently no experimental examples of $4d^2$ DPs, previous work on $5d^2$ systems has found evidence for both long-range ordered and alternative ground states. For example, a low-moment, long-range antiferromagnetic ground state has been reported for Ba_2CaOsO_6 [28], spin freezing without signs of long-range magnetic order has been found for Ca_2MgOsO_6 [29] and Ba_2YReO_6 [30], and a non-magnetic singlet ground state was proposed for $SrLaMgReO_6$ [31]. There are also many other $5d^2$ DPs that have not been characterized in detail. For example, there is no work on the magnetism of Sr_2YReO_6, and only one report on Sr_2InReO_6 that presents extremely limited information about its magnetic properties [32].

There is currently no consensus on the factors that contribute to ground state selection or their order of importance for $5d^2$ DPs. In this work, we make progress towards addressing this issue. We first revisit the crystal structures of the largely unexplored, $5d^2$ monoclinic DPs Sr_2YReO_6 and Sr_2InReO_6 with neutron powder diffraction and find that both systems crystallize in the $P2_1/n$ space group with no detectable B/B' site mixing. We then determine the magnetic ground states of these systems with a combination of magnetic susceptibility, heat capacity, neutron powder diffraction, and muon spin relaxation. Our combined measurements suggest that Sr_2YReO_6 is a spin glass; more specifically, the Re^{5+} moments freeze into a metastable configuration lacking long-range magnetic order. On the other hand, the Re^{5+} ions in Sr_2InReO_6 host a $J = 0$ non-magnetic singlet ground state. By making extensive comparisons between Sr_2YReO_6, Sr_2InReO_6, other $5d^2$ DPs, and Ni^{2+} $S = 1$ DPs, we propose that the diverse magnetic ground states of the $5d^2$ family arise from the combined effects of enhanced SOC, exchange interactions, and the great sensitivity of this particular d electron configuration to even modest structural distortions.

II. EXPERIMENTAL DETAILS

Polycrystalline $Sr_2B ReO_6$ (B = Y and In) samples were synthesized by a solid state reaction method. The starting materials of SrO, Y_2O_3 (or In_2O_3), Re and Re_2O_7 powders were weighed in an appropriate ratio and mixed thoroughly inside of a dry He glovebox. The homogeneous mixture was pelletized and transfered to a 5 ml Al_2O_3 crucible, which was then sealed in a vacuum quartz tube backfilled with 1/3 atmosphere of high-purity Ar. The ampoule was fired in a box furnace at 900°C for 48 hours. The fired pellets were reground, repelletized and then fired in a sealed quartz tube for another 100 hours. Room temperature x-ray powder diffraction was performed on a PANalytical X'Pert Pro MPD powder x-ray diffractometer using Cu $K_{\alpha 1}$ radiation and confirmed that the samples were of single phase. The DC magnetic susceptibilities were measured between 2-350 K using a Quantum Design (QD) magnetic property measurement system. The temperature dependence of the specific heat was measured between 2-200 K using a QD physical property measurement system.

Neutron powder diffraction (NPD) experiments were performed with 10 g of Sr_2YReO_6 and 10 g of Sr_2InReO_6 at Oak Ridge National Laboratory using the HB-2A powder diffractometer of the High Flux Isotope Reactor. Data was collected with neutron wavelengths of $\lambda = 1.54$ Å with collimation 12'-21'-12' and $\lambda = 2.41$ Å with collimation 12'-open-12'. The shorter wavelength provides greater intensity and higher Q coverage that was used to investigate the crystal structures, while the longer wavelength provides the lower Q coverage required for magnetic diffraction.

The μSR experiments were performed at the ISIS Pulsed Neutron and Muon Source, UK. We used the EMU and MuSR spectrometers in longitudinal geometry for investigating Sr_2InReO_6 (closed cycle refrigerator, base $T = 7.5$ K) and Sr_2YReO_6 (He-flow cryostat, base $T = 1.4$ K) respectively. In a typical μSR experiment spin-polarized muons are implanted into the sample, and they Larmor-precess around the local magnetic field at the muon stopping site [33]. Muons have a relatively short lifetime of 2.2 μs and decay into a position plus two neutrinos. The time-evolution of the muon spin polarization can be measured via a pair of opposing positron counters. This quantity is generally plotted as the asymmetry function, $A(t) = [N_1(t)\text{-}\alpha N_2(t)]/[N_1(t)+\alpha N_2(t)]$, where $N_{1,2}$ are the number of positron counts for the two detectors and α is a calibration parameter to correct for size and efficiency differences between the two detectors.

III. RESULTS

A. Crystal Structures

Figure 1 shows NPD data collected using $\lambda = 1.54$ Å for Sr_2YReO_6 and Sr_2InReO_6. Rietveld refinements were performed using FullProf [34]. Table I shows lattice constants and atomic fractional coordinates extracted from the NPD data, while Table II presents selected bond distances and angles. There is very little difference in any of the structural parameters between $T = 295$ and 4 K. Therefore, only the low temperature values are shown in most cases.

TABLE I: Lattice constants and atomic fractional coordinates for Sr_2YReO_6 and Sr_2InReO_6 extracted from the refinements of the $\lambda = 1.54$ Å neutron powder diffraction data.

(a) Sr_2YReO_6
Space group *P*2$_1$/*n*

Lattice parameters and refinement quality		
T	4 K	295 K
a	5.7779(1) Å	5.7892(1) Å
b	5.8193(1) Å	5.8123(1) Å
c	8.1698(1) Å	8.1970(1) Å
β	90.342(1)°	90.214(1)°
R_{wp}	4.74 %	5.30 %

Atom positions at T = 4 K				
Atom	Site	x	y	z
Sr	4e	0.5075(4)	0.5328(2)	0.2493(3)
Y	2c	0	0.5	0
Re	2d	0.5	0	0
O_1	4e	0.3021(4)	0.7277(4)	0.9594(3)
O_2	4e	0.4272(4)	0.9826(3)	0.2329(3)
O_3	4e	0.2318(4)	0.1986(4)	0.9619(3)

(b) Sr_2InReO_6
Space group *P*2$_1$/*n*

Lattice parameters and refinement quality		
T	4 K	295 K
a	5.6894(1) Å	5.7043(1) Å
b	5.7131(1) Å	5.7063(1) Å
c	8.0352(1) Å	8.0629(1) Å
β	89.808(1)°	89.921(1)°
R_{wp}	6.88 %	6.04 %

Atom positions at T = 4 K				
Atom	Site	x	y	z
Sr	4e	0.4940(7)	0.5281(3)	0.2503(6)
In	2c	0	0.5	0
Re	2d	0.5	0	0
O_1	4e	0.2968(6)	0.2835(6)	0.0385(5)
O_2	4e	0.2304(6)	0.7872(1)	0.0307(5)
O_3	4e	0.5701(5)	0.9871(4)	0.2366(4)

TABLE II: Selected bond distances (Å) and angles (deg) for Sr_2YReO_6 and Sr_2InReO_6 at $T = 4$ K extracted from the refinements of the $\lambda = 1.54$ Å neutron powder diffraction data.

	Sr_2YReO_6	Sr_2InReO_6
Re-O_1	1.981(2)	2.013(3)
Re-O_2	1.954(2)	1.972(3)
Re-O_3	1.957(2)	1.945(3)
Re-O_1-B	155.07(9)	154.92(13)
Re-O_2-B	155.98(10)	161.04(10)
Re-O_3-B	156.67(9)	157.11(13)

A previous x-ray powder diffraction report from 1969 [35] proposed that Sr_2YReO_6 crystallizes at room temperature in the cubic space group $Fm\bar{3}m$, but there are extra reflections in the NPD data that cannot be described by such a high crystal symmetry. Some of these additional Bragg peaks also rule out intermediate crystal symmetries (e.g. tetragonal) and monoclinic space groups with cell-centering (e.g. *I/2m and C2/c*). We instead find that the data refines best in the $P2_1/n$ space group, which is one of the most common structures for DPs. Sr_2InReO_6 was originally characterized as a $Fm\bar{3}m$ system [36] at room temperature also. However, recent work revisited the crystal structure and revised the room temperature space group to $P2_1/n$ [32], which is in good agreement with the current results. We find no evidence for a structural phase transition between 295 and 4 K in either material, as the data at 4 K also refines best in the $P2_1/n$ space group. We show diffraction data at both temperatures over a limited 2θ range in the insets of Fig. 1; there are small differences that arise from the enhanced monoclinic distortions with decreasing T.

The tolerance factor t is often used to characterize structural distortions in DPs, and it is defined as $t = (r_A + r_O)/(\sqrt{2}(r_{<B,B'>} + r_O))$ [8], where r_A and r_O are the ionic radii of A and O respectively, and $r_{<B,B'>}$ is the average ionic radius of B and B'. DPs with $t = 1$ or slightly greater are generally cubic, while the crystal symmetry decreases with decreasing t. Using values of ionic radii from Ref. [37], we find that Sr_2YReO_6 and Sr_2InReO_6 have tolerance factors of 0.94 and 0.97 respectively; these values are consistent with their monoclinic crystal symmetries. Finally, the Rietveld refinements confirm that there is essentially no site mixing between the Y/In and Re atomic positions for Sr_2YReO_6 and Sr_2InReO_6. These results are consistent with the large ionic radii differences between Y (0.9 Å) or In (0.8 Å) and Re (0.58 Å) [37]. We have also used NPD to confirm that there are no significant oxygen non-stoichiometries in these samples, consistent with expectations for synthesis in high-purity Ar gas, although we cannot rule out oxygen deficiency on the level of a few percent.

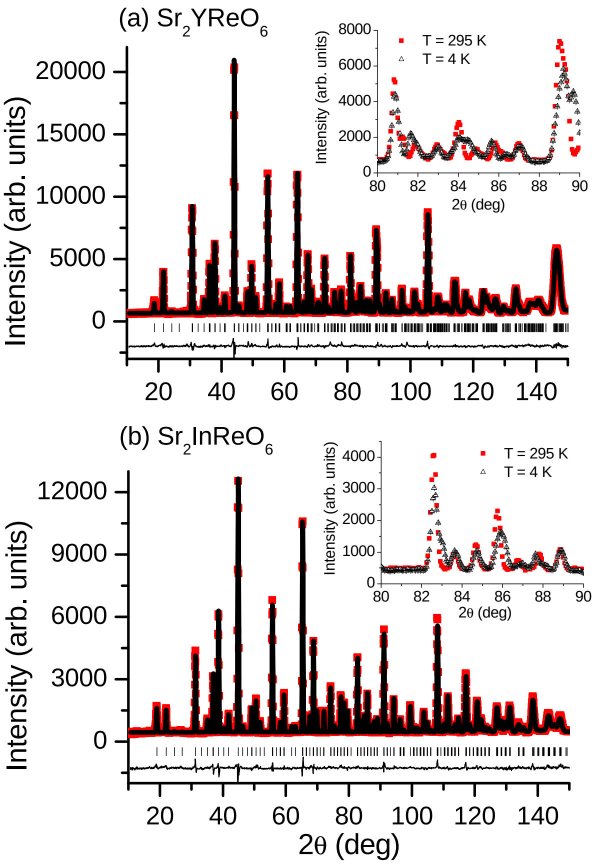

FIG. 1: Neutron powder diffraction measurements with a wavelength of 1.54 Å at $T = 295$ K for both (a) Sr_2YReO_6 and (b) Sr_2InReO_6. The corresponding structrual refinements are superimposed on the data. The insets show a comparison between the NPD data at $T = 295$ K and 4 K over a limited 2θ range.

B. Sr_2YReO_6: Magnetic Properties

Figure 2(a) and (b) depict the DC magnetic susceptibility measured in an applied field of $\mu_0 H = 0.1$ T, with $\chi = M/\mu_0 H$ (magnetization/applied field). The high temperature data is well-described by a Curie-Weiss law plus a constant, with a fit between 100 and 350 K yielding $\theta_{CW} =$ -382 K and an effective moment $\mu_{eff} = 1.92$ μ_B. The large, negative Curie-Weiss temperature is indicative of strong, dominant antiferromagnetic interactions. The magnitude of μ_{eff} is reduced from the $S = 1$ spin-only value of 2.83 μ_B, but consistent with reported values for other Re^{5+} DPs [30]. There are deviations from the Curie-Weiss law at low T; the zero-field-cooled (ZFC) and field-cooled (FC) datasets begin to diverge at 50 K, and the former also has a broad maximum at 12 K. A ZFC/FC divergence in χ with decreasing T is one common signature of a spin glass. In fact, the overall T-dependence of χ is reminiscent of previous results on the spin glass Sr_2CaReO_6 [24]. For that system, the temperature corresponding to the broad maximum in the ZFC χ data was

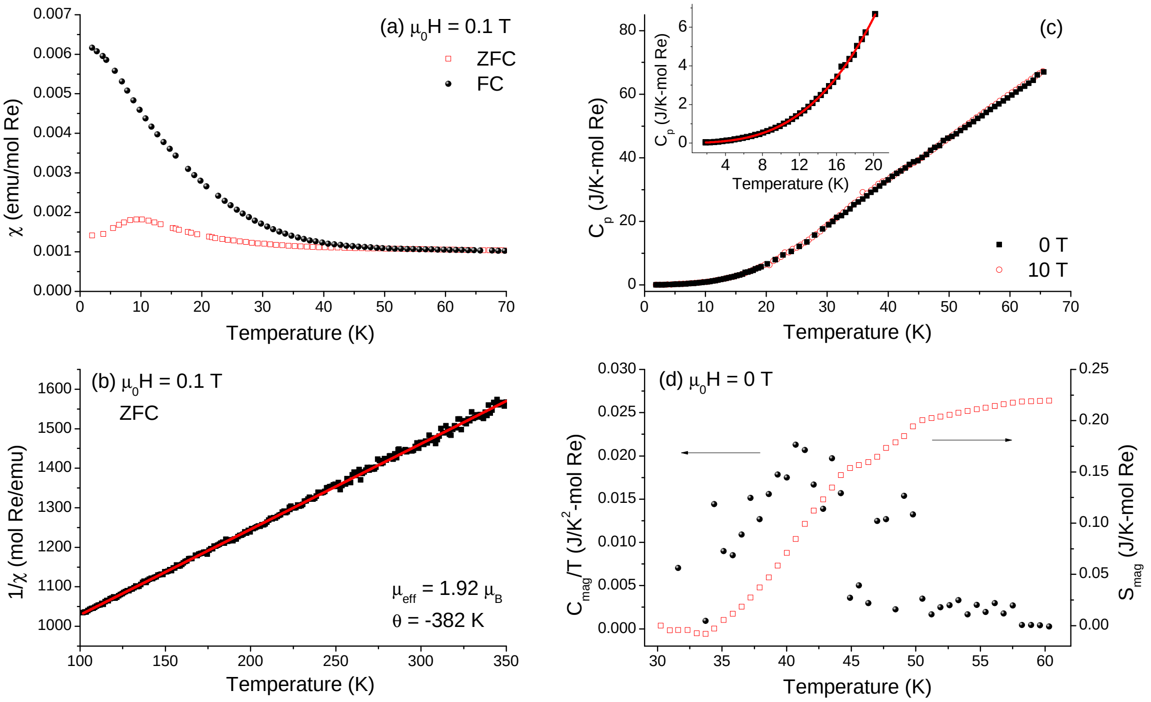

FIG. 2: (a) DC magnetic susceptibility χ of Sr_2YReO_6 measured in an applied field $\mu_0 H = 0.1$ T. Data collected under zero-field-cooled (ZFC) and field-cooled (FC) conditions diverges below 50 K. (b) The χ data fits well to a Curie-Weiss law plus a constant for $100 \leq T \leq 350$ K, with an effective moment $\mu_{eff} = 1.92\ \mu_B$ and a Curie-Weiss temperature of -382 K. (c) The heat capacity C_p of Sr_2YReO_6 for both $\mu_0 H = 0$ and 10 T. A weak, broad feature is visible in the data around 40 K, which likely has a magnetic origin as explained in the text. The inset shows the low-T C_p data in zero field, with the fit described in the text illustrated by a solid curve. (d) The magnetic contribution C_{mag} to C_p over the T-range 30-60 K. The entropy S_{mag} released over this entropy range is also indicated.

defined as the freezing temperature T_f; therefore we assume that $T_f = 12$ K in the present case. This assigned freezing temperature is supported by our μSR results presented later.

The heat capacity C_p of Sr_2YReO_6 is shown in Fig. 2(c) in fields of both 0 and 10 T. There is no clear λ anomaly indicative of long-range magnetic ordering and essentially no field dependence. The low temperature data ($T \leq 20$ K) fits well to the function $C_p = \gamma T + \beta T^3$ with $\gamma = 15.0(1)$ mJ/K^2-mol Re and $\beta = 0.774(5)$ mJ/K^4-mol Re. A non-zero γ is unexpected in insulators that exhibit magnetic order at low T, and this feature has been interpreted as a signature of spin glass behavior in insulating Sr_2MgReO_6 [25] and Li_4MgReO_6 [38]. Therefore, we assume that the linear component represents the magnetic contribution C_{mag}. Integrating C_{mag}/T up to the freezing temperature $T_f = 12$ K yields an entropy of 0.18 J/K-mol Re. Although this value represents only 2% of the expected entropy release for an $S = 1$ spin glass, the drastically-reduced value is consistent with reports of spin glassiness in Sr_2MgReO_6 (3% entropy release at T_f) [25], Li_4MgReO_6 (14% entropy release below T_f) [38] and the jarosite $(H_3O)Fe_3(SO_4)_2(OH)_6$ (6% entropy release at T_f) [39]. Furthermore, it is well-known that many spin glasses lose significant entropy above T_f [40].

An extremely weak and broad feature is visible in the higher temperature C_p data around 40 K, as shown in Fig. 2(c). This anomaly was assumed to have a magnetic origin for two reasons: (i) there is no change in the space group detected at temperatures below this feature in the NPD measurements and (ii) it corresponds well to the onset of the

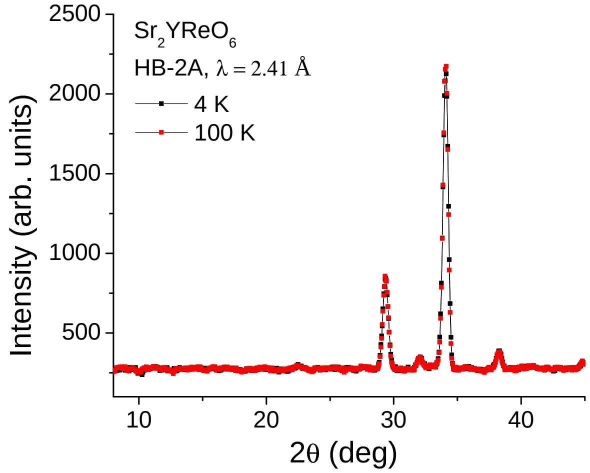

FIG. 3: Neutron powder diffraction measurements with a wavelength of 2.41 Å at $T = 4$ and 100 K for Sr_2YReO_6.

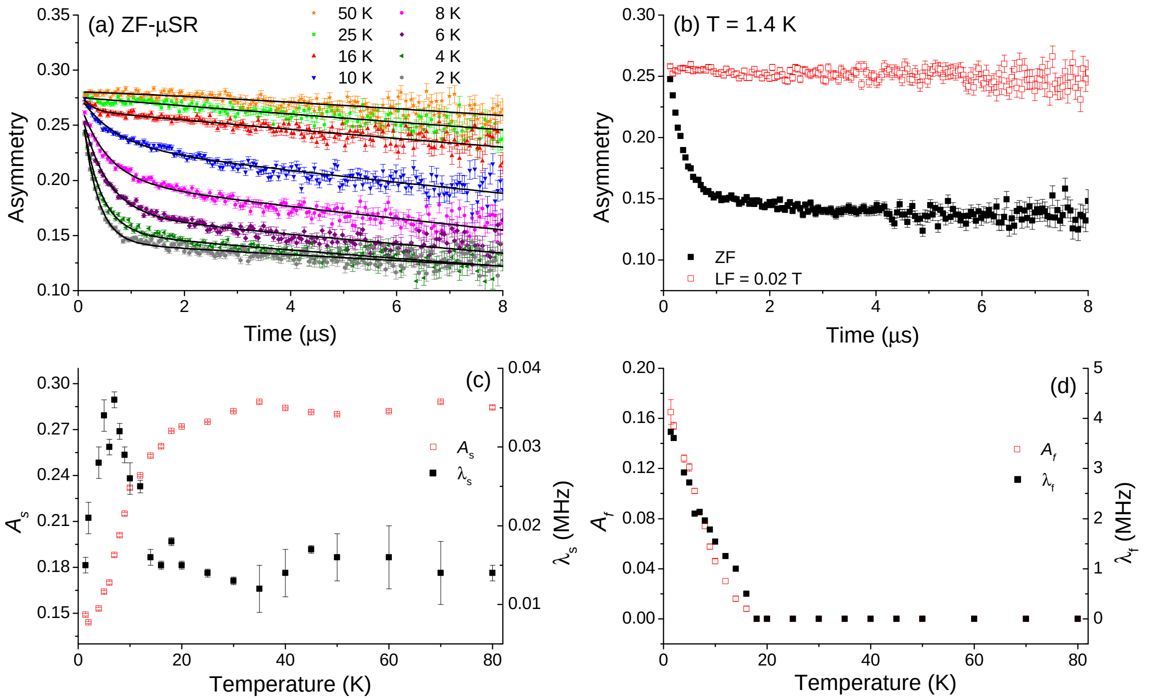

FIG. 4: (a) Zero field (ZF)-μSR spectra for Sr_2YReO_6 at selected temperatures. (b) ZF and longitudinal field (LF)-μSR results at $T = 1.4$ K. The ZF relaxation associated with the electron spins is completely decoupled in a modest field of 0.02 T, which suggests that it has a static origin. (c) T-dependence of the asymmetry and relaxation rate for the slow-relaxing component of the μSR spectra. (d) T-dependence of the asymmetry and relaxation rate for the fast-relaxing component of the μSR spectra.

ZFC/FC divergence in χ. We isolated this component by fitting the data between 30 and 60 K to a polynomial function and then subtracting off the fit as background. The result, plotted as C_{mag}/T, is shown in Fig. 2(d). There is a significant C_{mag} contribution over the T range 35-50 K. This feature, combined with the onset of the ZFC/FC divergence in χ at a similar temperature, are likely indicative of the presence of short-range magnetic correlations at temperatures higher than T_f. We note that the entropy released through the broad heat capacity anomaly is 0.22 J/K-mol Re, which is only an additional 2.5% of the total entropy release expected for an $S = 1$ spin glass. It is possible that additional entropy is released over a greater T range, but no other broad features are apparent in the raw C_p data.

Neutron powder diffraction data measured with a wavelength of 2.41 Å for Sr_2YReO_6 is depicted in Fig. 3 with $T = 4$ and 100 K. The two diffraction patterns are nearly identical, and therefore there is no evidence for long-range magnetic order in this data. This result is in sharp contrast to NPD results on $S = 1$ Ni^{2+} DPs, which always find evidence for a long-range ordered magnetic ground state with an ordered moment between 1.5-2.2 μ_B/Ni^{2+} [41–44]. The null diffraction result for Sr_2YReO_6 implies that the ordered Re moment is drastically-reduced as compared to its Ni counterparts or long-range order is absent down to 4 K. The former is possible due to increased covalency or enhanced spin-orbit coupling, and has been experimentally proven for Ba_2CaOsO_6 [28], where an ordered moment of $\sim 0.2\mu_B$ was estimated from muon spin relaxation (μSR) measurements.

The μSR technique [33] allows additional constraints to be placed on the possible magnetic ground state for Sr_2YReO_6. μSR is an extremely sensitive probe of magnetism and can readily differentiate between ordered, glassy, and dynamic ground states; ordered moments as small as 0.01 μ_B can be easily detected. Figure 4 summarizes μSR results collected with the MuSR spectrometer at ISIS. Figure 4(a) shows asymmetry spectra at selected temperatures measured in zero applied field (ZF). In the case of long-range magnetic order, an oscillatory signal with a frequency proportional to the local field at the muon site is the general expectation. However, if the local field from the ordered state is too large to be resolved at ISIS ($B_{loc} >$ 80 mT), then one should observe a significant loss in initial asymmetry instead. Neither of these features are visible in the spectra for Sr_2YReO_6 and therefore any scenario involving long-range magnetic order can be ruled out. Instead, we note that the data features two relaxing components comparable to those observed in the spin glass candidate Ba_2YReO_6 [30], and therefore the spectra were fit to a similar phenomenological function:

$$A(t) = A_s e^{-(\lambda_s t)^\beta} + A_f e^{-\lambda_f t} \tag{1}$$

where the first and second terms represent the slow and fast-relaxing components of the spectra respectively. Note that the slow-relaxing term consists of contributions from both the

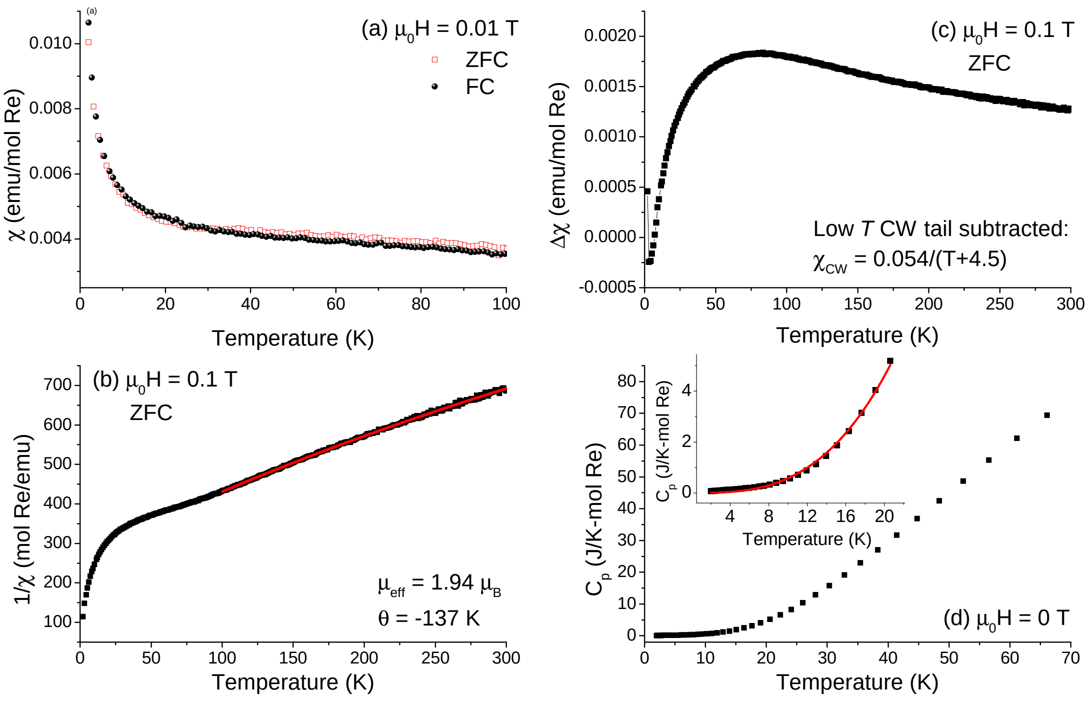

FIG. 5: (a) DC magnetic susceptibility χ of Sr$_2$InReO$_6$ measured in an applied field of $\mu_0 H = 0.01$ T. There is no evidence for magnetic ordering or ZFC/FC divergence down to 2 K. (b) The χ data ($\mu_0 H = 0.1$ T) fits well to a Curie-Weiss law plus a constant for $100 \leq T \leq 300$ K with an effective moment $\mu_{eff} = 1.94\ \mu_B$ and a Curie-Weiss temperature of -137 K. (c) $\Delta\chi$, obtained by subtracting a low-T Curie-Weiss tail (fitting range $T \leq 10$ K) likely arising from Re^{4+} impurities, shows a sharp drop with decreasing T. This is strong evidence for a non-magnetic singlet ground state in Sr$_2$InReO$_6$. (d) The heat capacity C_p of Sr$_2$InReO$_6$ for $\mu_0 H = 0$ T. No obvious magnetic features are visible in this data. The inset shows the low-T C_p data, with the fit described in the text illustrated by a solid curve.

sample and the sample holder. At the highest temperatures measured, only the first term was required in the fitting. Furthermore, β was found to decrease from ~ 1.5 at $T = 80$ K to 1 at $T = 30$ K, and therefore was subsequently fixed to 1 for $T < 30$ K. The decrease in β at lower temperatures is consistent with the slowing down of electron spins into the μSR time window; Gaussian relaxation due to static nuclear moments dominates at high temperature.

The fast component of the signal begins to develop just below 20 K as shown in Fig. 4(d); the relaxation rate λ_f and the amplitude A_f continue to increase down to 1.4 K. The T-dependence of the relaxation rate λ_s for the slow component depicted in Fig. 4(c) is drastically different, as λ_s reaches a maximum just below the assumed freezing temperature $T_f = 12$ K. A peak in the ZF μSR relaxation rate is commonly associated with spin freezing. This interpretation is consistent with the complete decoupling of the ZF relaxation in a relative modest longitudinal field (LF) of 0.02 T at $T = 1.4$ K as illustrated in Fig. 4(b), which implies a static local field distribution at the muon sites. More specifically, the longitudinal field results at $T = 1.4$ K indicate that the mean correlation time τ of the Re^{5+} moments in Sr$_2$YReO$_6$ is $> 10^{-6}$ s.

It is common to observe a two-component ZF-μSR relaxation function in spin glasses [24, 25] with the fast and slow relaxing terms corresponding to 2/3 and 1/3 of the total signal respectively. At $T = 1.4$ K, the ratio of A_s/A_f is close to 1. Assuming that about 25% of the muons stop in the sample holder, which is a reasonable value for the MuSR beamline based on previous work with a similar sample holder and slit sizes [45], and that this background contribution is included in the amplitude A_s, the relative contributions of the two relaxing components in the low T ZF-μSR spectra are consistent with expectations for a spin glass. Finally, it is interesting to note that μSR is insensitive to the short-range magnetic correlations of Sr$_2$YReO$_6$ over most of the temperature range between T_f and ~ 50 K where they are detected by other techniques, therefore the fluctuations of these spin clusters are likely characterized by a frequency outside the μSR time window in this regime.

C. Sr$_2$InReO$_6$: Magnetic Properties

Figure 5(a) depicts the DC magnetic susceptibility χ measured in an applied field of $\mu_0 H = 0.01$ T. There is no evidence for magnetic ordering or ZFC/FC divergence down to 2 K; the latter is in contrast to previous work which reports the onset of ZFC/FC divergence around 250 K [32]. While we cannot rectify the difference between our χ data and the earlier work, we repeated the χ measurements on our samples multiple times and found that all of the datasets were consistent with one another. Our high temperature data with $\mu_0 H = 0.1$ T is well-described by a Curie-Weiss law plus a constant, with a fit between 100 and 300 K yielding $\theta_{CW} =$ -137 K and an effective moment $\mu_{eff} = 1.94\ \mu_B$. While the effective moment has a similar value to Sr_2YReO_6, the Curie-Weiss temperature is significantly lower.

There are deviations from the high temperature Curie-Weiss law with decreasing T, with the appearance of another Curie-Weiss regime at the lowest temperatures measured. A fit to a Curie-Weiss law in the low-T regime ($T \leq 10$ K) yields $\mu_{eff} = 0.66\ \mu_B$ and $\theta_{CW} =$ -4.5 K. This contribution to χ likely arises from a small amount of Re^{4+} impurities in our sample, which may have been generated in the synthesis process due to a very small loss of oxygen not detectable by NPD. If we assume that each Re^{4+} carries an $S = 3/2$ moment, then the low T Curie-Weiss tail corresponds to $\sim$ 3% Re^{4+} impurities. Figure 5(c) shows $\Delta\chi$ vs T, which was obtained by subtracting the low-T Curie-Weiss tail from the raw χ data. The sharp drop in $\Delta\chi$ with decreasing T can be understood in the context of a non-magnetic singlet ground state for Sr_2InReO_6.

The specific heat C_p shown in Fig. 5(d) is consistent with this interpretation, as no λ anomaly characteristic of long-range ordering is observed at any temperature. Broad features are not apparent in the C_p data either, in contrast to observations for Sr_2YReO_6. Finally, although the low T C_p data ($T \leq 20$ K) still fits well to the function $C_p = \gamma T + \beta T^3$ with $\gamma = 0.667(3)$ mJ/K^2-mol Re and $\beta = 0.57(1)$ mJ/K^4-mol Re, the magnitude of γ is significantly reduced compared to Sr_2YReO_6. This finding is suggestive that the magnetic ground states of Sr_2YReO_6 and Sr_2InReO_6 are fundamentally different, although it is important to note that β and γ are very sensitive to the exact choice of fitting range. If we extend the low-T fit for Sr_2InReO_6 up to 35 K, then we obtain similar β and γ parameters as reported in Ref. [32]. In general, our C_p data is in excellent agreement with that work.

Neutron powder diffraction data with a wavelength of 2.41 Å for Sr_2InReO_6 is depicted in Fig. 6 with $T = 4$ and 100 K respectively. Similarly to the case of Sr_2YReO_6, the two diffraction patterns are nearly identical, and therefore there is no evidence for long-range magnetic order in this data either. The null diffraction result has similar implications to the Sr_2YReO_6 case: either the ordered Re moment is drastically-reduced as compared to its Ni counterparts or long-range order is absent down to 4 K.

μSR proved to be useful here also for differentiating between these possibilities. Figure 7 summarizes μSR results collected with the EMU spectrometer at ISIS. Figure 7(a) shows ZF-μSR asymmetry spectra at $T = 7.5$ and 16 K. No missing asymmetry or spontaneous oscillations, as would be expected for a long-range ordered ground state, are apparent in the data. Instead, the spectra shows weak relaxation at all temperatures and can be fit well to the following function:

$$A(t) = Ae^{-(\lambda t)^{\beta}} \tag{2}$$

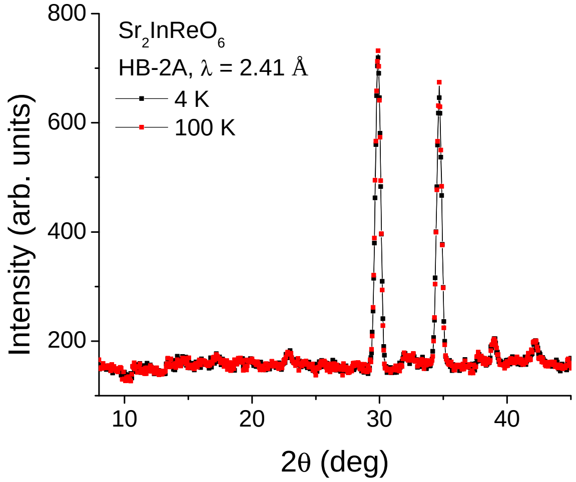

FIG. 6: Neutron powder diffraction measurements with a wavelength of 2.41 Å at $T = 4$ and 100 K for Sr_2InReO_6.

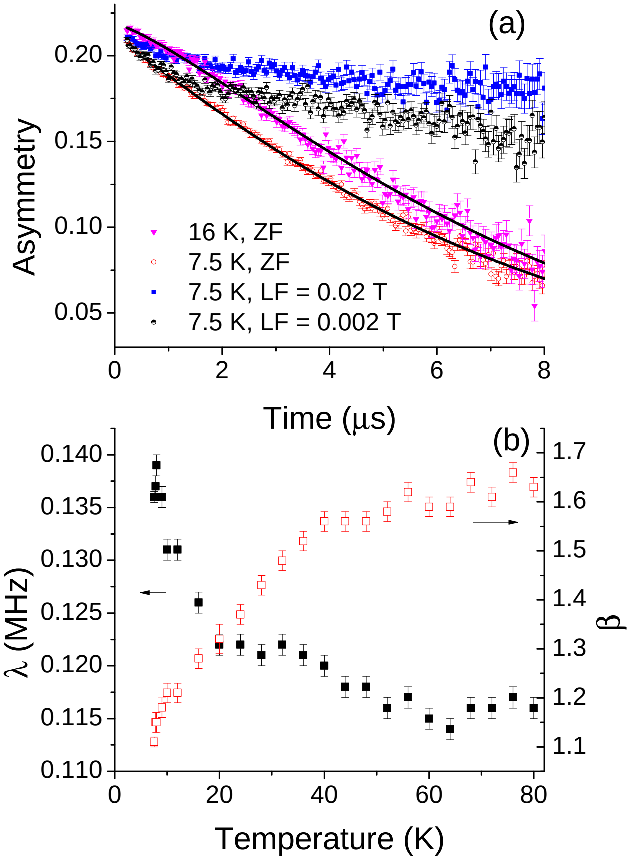

FIG. 7: (a) ZF and LF-μSR spectra for Sr_2InReO_6 at selected temperatures. Most of the observed relaxation is due to static nuclear moments, although a very small quasi-static electronic component develops at low T. (b) T-dependence of the relaxation rate λ and power β for the ZF-μSR spectra.

The fitting results for λ and β are shown in Fig. 7(b). At the highest temperatures measured $\beta \to 2$ and $\lambda \to 0.115$ μs^{-1}, which are consistent with expectations that the dominant relaxation mechanism in this regime arises from randomly-oriented, static nuclear moments. With decreasing T, $\beta \to 1$ and λ shows a monotonic increase corresponding to an overall change smaller than the absolute value at high T; this is precisely the behavior expected for a dilute, quasi-static electron spin system [33]. The LF-μSR spectra shown in Fig. 7(a) are in good agreement with this interpretation, as the ZF relaxation at $T = 7.5$ K is significantly decoupled even in a modest applied LF of 0.002 T. Overall, the μSR data provides additional support for the formation of a non-magnetic singlet state for the Re^{5+} spins at low T, which coexists with a small fraction of quasi-static free spins. We note that our μSR data for Sr_2InReO_6 looks qualitatively similar to μSR data for other proposed singlet ground state DPs, including Ba_2YMoO_6 [22, 23] and $SrLaMgReO_6$ [31].

IV. DISCUSSION

We have firmly established that Sr_2YReO_6 hosts a spin-glass ground state, while Sr_2InReO_6 is characterized by a non-magnetic singlet ground state instead. Here, we make an effort to understand how the magnetic ground states of d^2 DPs evolve as a function of various tuning parameters, including spin-orbit coupling, structural distortions, and exchange interactions. There have now been several experimental reports in the literature describing the magnetic properties of particular members of this family, but an overall unifying picture is lacking. There are two different types of d^2 DPs, which are based on Os^{6+} or Re^{5+}. There are no known d^2 DPs consisting of $3d$ or $4d$ transition metals, so the closest available comparison arises from considering Ni^{2+} $S = 1$ systems, with the caveat that the active orbitals in the case of Ni^{2+} are e_g and not t_{2g}. Table III summarizes several properties of various $5d^2$ and Ni^{2+} $S = 1$ DPs, including the space group SpG, the tolerance factor t, the Curie-Weiss temperature θ_{CW}, the ordering or freezing temperature $T_{c/f}$, and the magnetic ground state.

Some trends in Table III are readily apparent. Long-range ordered ground states are found for all of the Ni^{2+} DP compounds previously investigated, with the type of long-range order determined by the signs and relative magnitudes of nearest neighbor (NN) exchange J_1 and next-nearest neighbor (NNN) exchange J_2. On the other hand, the magnetic ground states for the $5d$ transition metal-based compounds are extremely varied. The $5d$ systems with higher crystal symmetry show an increased tendency to exhibit magnetic order, while the lower symmetry systems are generally characterized by spin-glass or non-magnetic singlet ground states. On the basis of these observations alone, one obvious conclusion is that introducing enhanced spin-orbit coupling combined with significant structural distortions away from the ideal fcc lattice leads to a destabilization of magnetic order in this family. This finding is somewhat counterintuitive, as the geometric frustration generally argued to be responsible for the lack of long-range magnetic order in d^2 DPs should be maximized in cubic systems.

A detailed understanding of the single ion ground state for $5d^2$ systems is essential to understand this puzzling trend. The $5d^2$ ions of cubic DPs are in an ideal octahedral oxygen environment, which leads to a very large t_{2g}/e_g splitting Δ. To satisfy Hund's first rule, the total spin for the two electrons is $S = 1$. The orbital triplet degree of freedom must also be taken into account to determine the single ion ground state for a d^2 system, as orbital angular momentum L is generally not quenched in $5d$ magnets. If Hund's coupling $J_H \geq 2\lambda_{SO}$, one finds that spin and orbital moments lock together to create a $J = 2$ ground state [27, 46, 47].

TABLE III: Structural and magnetic properties of selected $3d$ $S = 1$ and $5d^2$ double perovskite systems with a single magnetic sublattice

Compound	SpG	t	θ_{CW}	$T_{c/f}$	Ground state	Ref.
Ba_2WNiO_6	$Fm\bar{3}m$	1.05	?	?	Type-II AF	[41]
Sr_2WNiO_6	$I4/m$	0.99	-175	54	AFLRO	[54]
Sr_2TeNiO_6	$C2/m$	1	-240	28-35	AFLRO	[54]
La_2TiNiO_6	$P2_1/n$	0.96	-130	25	Type-II AF	[42]
$SrLaSbNiO_6$	$P2_1/n$	0.97	?	26	Type-I AF	[43]
Ca_2WNiO_6	$P2_1/n$	0.95	-100	50	Type-II AF	[44]
Ba_2CaOsO_6	$Fm\bar{3}m$	0.99	-156	50	AFLRO	[28]
Sr_2MgOsO_6	$I4/m$	1	-347	110	AFLRO	[29]
Ca_3OsO_6	$P2_1/n$	0.9	-151	50	AFLRO?	[55]
Ca_2MgOsO_6	$P2_1/n$	0.96	-72	19	SG	[29]
Ba_2YReO_6	$Fm\bar{3}m$	1	-616	50	SG	[30]
Sr_2YReO_6	$P2_1/n$	0.94	-382	12	SG	this work
La_2LiReO_6	$P2_1/n$	0.95	-204	50	SG/SS?	[30]
$SrLaMgReO_6$	$P2_1/n$	0.97	-161	-	SS	[31]
Sr_2InReO_6	$P2_1/n$	0.97	-137	-	SS	this work

The acronyms for the magnetic ground states specified in the table mean the following: AF (antiferromagnet), AFLRO (unknown antiferromagnetic long-range order), SG (spin glass), SS (non-magnetic singlet state). θ_{CW} and $T_{c/f}$ are both presented in K.

In lower symmetry $5d^2$ DPs, the five-fold degeneracy of the $J = 2$ multiplet can be removed by a non-cubic crystal field term δ, which is defined here as the energy difference between the ground state and the lowest-lying excited state. A non-magnetic singlet ground state ($J = 0$) is even possible in principle for a significant δ, due to the integer value for the angular momentum of the cubic crystal field ground state. In fact, recent RIXS work on Na_2IrO_3 [48] and Sr_3CuIrO_6 [49] has proven that even modest structural distortions leading to non-cubic crystal fields at the Ir^{4+} sites can induce large intramultiplet splitting on the order of 100's of meVs in $5d$ magnets. Furthermore, non-cubic crystal field splitting has been argued to play an important role in stabilizing the ordered magnetic ground state for the $5d^4$ DP Sr_2YIrO_6 [50], since a non-magnetic single ion singlet state is expected for a cubic d^4 system in the strong SOC limit.

The enhanced sensitivity of $5d$ systems to small structural distortions, as compared to their $3d$ counterparts, arises from the spatially-extended nature of the $5d$ orbitals. We propose here that this difference is one of the key factors leading to a wide variation of magnetic ground states for $5d^2$ DPs. If $\delta = 0$, which is valid for cubic systems, then the five-fold degeneracy of the $J = 2$ multiplet will be preserved and a long-range ordered magnetic ground state will be the most common outcome [27]. On the other hand, if the intramultiplet splitting δ for the non-cubic systems becomes significant and creates a singlet ground state, there are three main possibilities based on the strength of the exchange interactions J_{ex} between the magnetic ions. It is well-known that there is a critical value $x_c = (J_{ex}/\delta)_c$ above which magnetic moments are induced in singlet systems [51] and typical long-range magnetic order can still arise. On the other hand, for $x_c > J_{ex}/\delta$, spontaneous magnetism becomes impossible and therefore non-magnetic singlet ground states are realized instead. The third case with $x_c \approx J_{ex}/\delta$ proposed for the spin glass $PrAu_2Si_2$ is perhaps the most interesting, as it has been suggested that the spin freezing results from dynamic fluctuations of the crystal-field levels that destabilize the induced moments and frustrate the development of long-range magnetic order [51]. This mechanism can serve as the source of both the frustration and disorder that are generally accepted to be essential ingredients in all spin glasses, and it can provide a natural explanation for why no obvious source of disorder has ever been found in $5d^2$ spin glass DPs.

Magnetic characterization studies of $5d^2$ DPs yield results that are broadly consistent with our explanation given above for magnetic ground state selection. We first consider Sr_2YReO_6 and Sr_2InReO_6, which were extensively characterized in the present work. The Re^{5+} sites of both systems are subjected to non-cubic crystal fields; this deviation from ideal fcc lattice geometry simultaneously enhances δ and reduces J_{ex}. One way to roughly quantify the former effect is by considering Re-O bond lengths. At $T = 4$ K, our NPD measurements yield three inequivalent Re-O bond lengths of 1.95, 1.96, and 1.98 Å and 1.94, 1.97, and 2.01 Å for the Y and In systems respectively. The latter effect can also be quantified by considering the magnitude of the Curie-Weiss temperatures θ_{CW}. Based on the significantly reduced value of θ_{CW} coupled with the enhanced structural distortion for Sr_2InReO_6 relative to Sr_2YReO_6, it is not surprising for a $J = 0$ single ion ground state to arise for the former but not for the latter.

In general, Table III indicates that $5d^2$ cubic systems with low Curie-Weiss temperatures and significant structural distortions tend to exhibit singlet ground states, while cubic systems show an increased tendency for magnetic order. Ba_2YReO_6 is the one known example of a cubic $5d^2$ system that does not show long-range order. However, broad magnetic Bragg peaks were recently observed that are characteristic of a cluster spin glass [52], which may indicate that this system is proximate to a quantum phase transition into a long-range ordered state. Indeed, it is possible that Ba_2YReO_6 is not an ideal fcc system but rather exhibits a small structural distortion that can best be observed by synchrotron x-ray diffraction.

Finally, we note that our discussion for $5d^2$ systems does not extend to $4d^1$/$5d^1$ systems since they cannot have single ion singlet ground states according to Kramer's theorem. On the basis of enhanced quantum fluctuations and strong geometric frustration, theoretical work for d^1 systems predicts that exotic collective spin-singlet ground states including quantum spin liquids and valence bond solids/glasses can be realized [53]. While we cannot rule out similar origins for the singlet ground states in $5d^2$ DPs, previous theoretical work on these systems indicates that simple ordered states dominate the phase diagram instead [27].

V. CONCLUSIONS

We have performed detailed characterization studies of the $5d^2$ double perovskites Sr_2InReO_6 and Sr_2YReO_6. Both systems crystallize in the space group $P2_1/n$ and therefore non-cubic crystal fields are present at the Re^{5+} sites. Our combined magnetic susceptibility, heat capacity, neutron powder diffraction, and muon spin relaxation measurements suggest that Sr_2YReO_6 is a spin glass while Sr_2InReO_6 is best characterized by a non-magnetic singlet ground state. We attribute the great diversity of magnetic ground states found for the $5d^2$ double perovskite family, including the different ground states for Sr_2YReO_6 and Sr_2InReO_6 determined in this work, to a subtle interplay between spin-orbit coupling, non-cubic crystal fields, and exchange interactions. To verify our hypothesis for ground state selection in $5d^2$ systems, it will be important to systematically determine the crystal field level schemes and exchange interactions for several members of this family.

We thank C.M. Thompson and M.A. McGuire for useful discussions. This research was supported by the US Department of Energy (DOE), Office of Basic Energy Sciences. A.A.A. and S.C. were supported by the Scientific User Facilities Division, and J.-Q.Y. was supported by the Materials Science and Engineering Division. Z.Y.Z. acknowledges the CEM, and NSF MRSEC, under grant DMR-1420451. The neutron diffraction experiments were performed at the High Flux Isotope Reactor, which is sponsored by the Scientific User Facilities Division.

---

[*] author to whom correspondences should be addressed: E-mail:[aczelaa@ornl.gov]

[1] W. Witczak-Krempa, G. Chen, Y.B. Kim, and L. Balents, Annu. Rev. Condens. Matter Phys. **5**, 57 (2014).

[2] B.J. Kim, H. Jin, S.J. Moon, J.-Y. Kim, B.-G. Park, C.S. Leem, J. Yu, T.W. Noh, C. Kim, S.-J. Oh, J.-H. Park, V. Durairaj, G. Cao, and E. Rotenberg, Phys. Rev. Lett. **101**, 076402 (2008).

[3] F. Wang and T. Senthil, Phys. Rev. Lett. **106**, 136402 (2011).

[4] B.-J. Yang and Y.B. Kim, Phys. Rev. B **82**, 085111 (2010).

[5] D. Pesin and L. Balents, Nature Physics **6**, 376 (2010).

[6] J.-M. Carter, V.V. Shankar, M.A. Zeb, and H.-Y. Kee, Phys. Rev. B **85**, 115105 (2012).

[7] G. Jackeli and G. Khaliullin, Phys. Rev. Lett. **102**, 017205 (2009).

[8] S. Vasala and M. Karppinen, Progress in Solid State Chemistry **43**, 1 (2015).

[9] G.-X. Cao, A. Subedi, S. Calder, J.-Q. Yan, J. Yi, Z. Gai, L. Poudel, D.J. Singh, M.D. Lumsden, A.D. Christianson, B.C. Sales, and D. Mandrus, Phys. Rev. B **87**, 155136 (2013).

[10] A.M. Cook, S. Matern, C. Hickey, A.A. Aczel, and A. Paramekanti, Phys. Rev. B **92**, 020417(R) (2015).

[11] A.A. Aczel, A.M. Cook, T.J. Williams, S. Calder, A.D. Christianson, G.-X. Cao, D. Mandrus, Y.B. Kim, and A. Paramekanti, arXiv: 1604.08431 (unpublished).

[12] P.D. Battle, J.B. Goodenough and R. Price, Journal of Solid State Chemistry **46**, 234 (1983).

[13] P.D. Battle and W.J. Macklin, Journal of Solid State Chemistry **52**, 138 (1984).

[14] P.D. Battle and C.W. Jones, Journal of Solid State Chemistry **78**, 108 (1989).

[15] P.D. Battle, C.P. Grey, M. Hervieu, C. Martin, C.A. Moore and Y. Paik, Journal of Solid State Chemistry **175**, 20 (2003).

[16] E. Kermarrec, C.A. Marjerrison, C.M. Thompson, D.D. Maharaj, K. Levin, S. Kroeker, G.E. Granroth, R. Flacau, Z. Yamani, J.E. Greedan, and B.D. Gaulin, Phys. Rev. B **91**, 075133 (2015).

[17] A.E. Taylor, R. Morrow, D.J. Singh, S. Calder, M.D. Lumsden, P.M. Woodward, and A.D. Christianson, Phys. Rev. B **91**, 100406(R) (2015).

[18] A.A. Aczel, D.E. Bugaris, L. Li, J.-Q. Yan, C. de la Cruz, H.-C. zur Loye, and S.E. Nagler, Phys. Rev. B **87**, 014435 (2013).

[19] A.A. Aczel, P.J. Baker, D.E. Bugaris, J. Yeon, H.-C. zur Loye, T. Guidi, and D.T. Adroja, Phys. Rev. Lett. **112**, 117603 (2014).

[20] K. Lefmann and C. Rischel, Eur. Phys. J. B **21**, 313 (2001).

[21] A.E. Taylor, R. Morrow, R.S. Fishman, S. Calder, A.I. Kolesnikov, M.D. Lumsden, P.M. Woodward, and A.D. Christianson, arXiv: 1511.07486v2 (unpublished).

[22] M.A. de Vries, A.C. Mclaughlin, and J.-W.G. Bos, Phys. Rev. Lett. **104**, 177202 (2010).

[23] T. Aharen, J.E. Greedan, C.A. Bridges, A.A. Aczel, J. Rodriguez, G. MacDougall, G.M. Luke, T. Imai, V.K. Michaelis, S. Kroeker, H. Zhou, C.R. Wiebe, and L.M.D. Cranswick, Phys. Rev. B **81**, 224409 (2010).

[24] C.R. Wiebe, J.E. Greedan, G.M. Luke, and J.S. Gardner, Phys. Rev. B **65**, 144413 (2002).

[25] C.R. Wiebe, J.E. Greedan, P.P. Kyriakou, G.M. Luke, J.S. Gardner, A. Fukaya, I.M. Gat-Malureanu, P.L. Russo, A.T. Savici, and Y.J. Uemura, Phys. Rev. B **68**, 134410 (2003).

[26] J.E. Greedan, S. Derakhshan, F. Ramezanipour, J. Siewenie, and Th. Proffen, J. Phys. Condens. Matter **23**, 164213 (2011).

[27] G. Chen and L. Balents, Phys. Rev. B **84**, 094420 (2011).

[28] C.M. Thompson, J.P. Carlo, R. Flacau, T. Aharen, I.A. Leahy, J.R. Pollichemi, T.J.S. Munsie, T. Medina, G.M. Luke, J. Munevar, S. Cheung, T. Goko, Y.J. Uemura, and J.E. Greedan, J. Phys.: Condens. Matter **26**, 306003 (2014).

[29] Y. Yuan, H.L. Feng, M.P. Ghimire, Y. Matsushita, Y. Tsujimoto, J. He, M. Tanaka, Y. Katsuya, and K. Yamaura, Inorg. Chem. **54**, 3422 (2015).

[30] T. Aharen, J.E. Greedan, C.A. Bridges, A.A. Aczel, J. Rodriguez, G. MacDougall, G.M. Luke, V.K. Michaelis, S. Kroeker, C.R. Wiebe, H. Zhou, and L.M.D. Cranswick, Phys. Rev. B **81**, 064436 (2010).

[31] C.M. Thompson, L. Chi, J.R. Hayes, A.M. Hallas, M.N. Wilson, T.J.S. Munsie, I.P. Swainson, A.P. Grosvenor, G.M. Luke, and J.E. Greedan, Dalton Trans. **44**, 10806 (2015).

[32] H. Gao, A. Llobet, J. Barth, J. Winterlik, C. Felser, M. Panthofer, and W. Tremel, Phys. Rev. B **83**, 134406 (2011).

[33] P.D. de Reotier and A. Yaouanc, J. Phys.: Condens. Matter **9**, 9113 (1997).

[34] J. Rodriguez-Carvajal, Physica B **192**, 55 (1993).

[35] G. Baud and M. Capestan, Bulletin de la Societe Chimique de France **1969**, 1872 (1969).

[36] A.W. Sleight, J. Longo, and R. Ward, Inorg. Chem. **1**, 245 (1962).

[37] R.D. Shannon, Acta Crystallographica **A32**, 751 (1976).

[38] M. Bieringer, J.E. Greedan, and G.M. Luke, Phys. Rev. B **62**, 6521 (2000).

[39] A.S. Wills, A. Harrison, S.A.M. Mentink, T.E. Mason, and Z. Tun, Europhys. Lett. **42**, 325 (1998).

[40] J.A. Mydosh, *Spin Glasses, An Experimental Introduction* (Taylor & Francis, London, 1993).

[41] D.E. Cox, G. Shirane, and B.C. Frazer, Journal of Applied Physics **38**, 1459 (1967).

[42] E. Rodriguez, M.L. Lopez, J. Campo, M.L. Veiga, and C. Pico, J. Mater. Chem. **12**, 2798 (2002).

[43] M.P. Attfield, P.D. Battle, S.K. Bollen, T.C. Gibb, and R.J. Whitehead, Journal of Solid State Chemistry **100**, 37 (1992).

[44] K.R. Chakraborty, A. Das, P.S.R. Krishna, S.M. Yusuf, S.J. Patwe, S.N. Achary, and A.K. Tyagi, Journal of Alloys and Compounds **457**, 15 (2008).

[45] A.A. Aczel, L. Li, V.O. Garlea, J.-Q. Yan, F. Weickert, V.S. Zapf, R. Movshovich, M. Jaime, P.J. Baker, V. Keppens, and D. Mandrus, Phys. Rev. B **92**, 041110(R) (2015).

[46] K.W. Plumb, A.M. Cook, J.P. Clancy, A.I. Kolesnikov, B.C. Jeon, T.W. Noh, A. Paramekanti, and Y.-J. Kim, Phys. Rev. B **87**, 184412 (2013).

[47] A. Cook and A. Paramekanti, Phys. Rev. B **88**, 235102 (2013).

[48] H. Gretarsson, J.P. Clancy, X. Liu, J.P. Hill, E. Bozin, Y. Singh, S. Manni, P. Gegenwart, J. Kim, A.H. Said, D. Casa, T. Gog, M.H. Upton, H.-S. Kim, J. Yu, V.M. Katukuri, L. Hozoi, J. van den Brink, and Y.-J. Kim, Phys. Rev. Lett. **110**, 076402 (2013).

[49] X. Liu, V.M. Katukuri, L. Hozoi, W-G. Yin, M.P.M. Dean, M.H. Upton, J. Kim, D. Casa, A. Said, T. Gog, T.F. Qi, G. Cao, A.M. Tsvelik, J. van den Brink, and J.P. Hill, Phys. Rev. Lett. **109**, 157401 (2012).

[50] G. Cao, T.F. Qi, L. Li, J. Terzic, S.J. Yuan, L.E. DeLong, G. Murthy, and R.K. Kaul, Phys. Rev. Lett. **112**, 056402 (2014).

[51] E.A. Goremychkin, R. Osborn, B.D. Rainford, R.T. Macaluso, D.T. Adroja, and M. Koza, Nature Physics **4**, 766 (2008).

[52] C.M. Thompson, private communication.

[53] G. Chen, R. Pereira, and L. Balents, Phys. Rev. B **82**, 174440 (2010).

[54] D. Iwanaga, Y. Inaguma, and M. Itoh, Materials Research Bulletin **35**, 449 (2000).

[55] H.L. Feng, Y. Shi, Y. Guo, J. Li, A. Sato, Y. Sun, X. Wang, S. Yu, C.I. Sathish, and K. Yamaura, Journal of Solid State Chemistry **201**, 186 (2013).